Scaling laws of passive tracer dispersion in the turbulent surface layer.

Alex Skvortsov,* Milan Jamriska, and Timothy C. DuBois
Defence Science and Technology Organisation, 506 Lorimer Street, Fishermans Bend, Vic 3207, Australia
(Dated: July 29, 2011)

Experimental results for passive tracer dispersion in the turbulent surface layer under stable conditions are presented. In this case, the dispersion of tracer particles is determined by the interplay of three mechanisms: relative dispersion (celebrated Richardson's mechanism), shear dispersion (particle separation due to variation of the mean velocity field) and specific surface-layer dispersion (induced by the gradient of the energy dissipation rate in the turbulent surface layer). The latter mechanism results in the rather slow (ballistic) law for the mean squared particle separation. Based on a simplified Langevin equation for particle separation we found that the ballistic regime always dominates at large times. This conclusion is supported by our extensive atmospheric observations. Exit-time statistics are derived from the experimental dataset and show a reasonable match with the simple dimensional asymptotes for different mechanisms of tracer dispersion, as well as predictions of the multifractal model and experimental data from other sources.

PACS numbers: 47.27.nb, 47.27.eb, 64.60.al, 05.45.Tp, 92.60.Fm, 92.60.Mt

I. INTRODUCTION

The phenomenon of scalar turbulence or random advection of tracer particles by random turbulent flow has become a topic of significant attention during the last few years [1], [2], [3], [4], [5], [6], [7]. This is not only due to its significance for understanding the transport processes in global geophysical systems (e.g. the atmosphere and oceans) and as a theoretical framework for the design of some technological applications (mixers, chemical reactors, combustion chambers), but is perhaps even more important as an instructive example of modern methods of theoretical physics applied to a highly non-equilibrium dynamic system in order to deduce new phenomenology and a wealth of analytical results that can be validated numerically and experimentally. Known examples are: analytical scaling for white-noise scalar turbulence (solutions of the Kraichnan model [1], [2], [3]); application of conformal invariance to the two-dimensional tracer flow [4]; re-normalization group formalism; multi-fractal structure of tracer statistics [1] and others (see review [8] and references therein). Remarkably, the recent applications of the theoretical framework for this phenomena provide rigorous ways to overcome the initially restrictive assumptions of the underlying model of locally isotropic turbulence by incorporating effects of anisotropy, flow boundaries, mean velocity shear, buoyancy, etc. and enable the analytical calculations of associated corrections [9], [5], [10].

In this paper we report our experimental results on the dispersion of passive tracers in the turbulent surface layer. The wall-bounded turbulent flow provides flexible settings to study the effects of mean velocity shear (i.e. non-uniform wind) and system boundaries (the underlying surface) on the passive scalar dispersion.

* alex.skvortsov@dsto.defence.gov.au

The celebrated Richardson law [11] established the growth of the mean inter-particle distance:

$$\langle R^2(t)\rangle \sim \lambda t^n, \tag{1}$$

where $n = 3$, λ is a scale-independent dimensional parameter, and became a signature of turbulent dispersion (see review [12]). It was later recognized by Oboukhov and Corsin that this law is a direct consequence of Kolmogorov scaling in turbulence [13], [3]. Indeed, from a power-law assumption for the velocity differences $\delta v \sim dR/dt \propto R^h$ and (1) it is easily to derive $R \propto t^{\frac{1}{1-h}}$ or $h = 1 - 2/n$. The latter expression leads to the Richardson law with $\langle R^2(t)\rangle \propto t^3$ for the Kolmogorov scaling $h = 1/3$. This is a reflection of an intimate and well-known connection between the power exponent of the particle separation law n in (1) and the passive tracer statistics [3]. From a mathematical point of view, this connection can be translated into a scaling law of the correlation functions of the tracer concentration that includes the parameter n [13], [3]:

$$S_2(R) = 2[F_2(0) - F_2(R)] \propto R^{2/n}, \quad n = 1/(1-h), \tag{2}$$

where

$$F_2(R) = \langle C(\mathbf{x}+\mathbf{R},t)C(\mathbf{x},t)\rangle \tag{3}$$

is the pair-correlation function.

Different values of n (the scaling exponent of the mean squared displacement) have been derived theoretically and experimentally for different kinds of turbulent flow (see [12], [6] and refs therein). Contrarily, a particular value of n can be associated with a particular energy injection mechanism of turbulence and can be used for characterization of its dispersive properties. As was mentioned above, for the tracer dispersion by Kolmogorov (locally isotropic) turbulence, $n = 3$ (Richardson law). For Bolgiano-Obukhov (buoyancy dominated) turbulence, $n = 5$ [10]. For turbulence with mean velocity shear it was recently deduced [6] that $n = 6$ (for

particle separation along the mean velocity) and $n = 4$ (for separation in the transverse direction). It is worth noting that in all latter cases the separation of particles is always faster than in the standard Richardson regime (i.e. without velocity shear). For surface layer turbulence (i.e. turbulent motion near a flow boundary), whose scaling properties are significantly different from the isotropic Kolmogorov model, the value of n can eventually deviate from Richardson's prediction. Particularly, the self-similarity arguments applying to this case lead to much lower values of the scaling exponent of the mean squared displacement ($n = 2$ or so-called "ballistic" regime, since $R \propto t$) [14]. Finally, for the "combined" case (turbulent flow near a boundary *and* a mean velocity shear) Ref [9] argues that there is no universal value for the parameter h in (2) (and hence neither for exponent n).

From simple dimensional analysis it is obvious that the dimensional parameter λ in (1) should also be different for the different values of n, i.e. for the particular type of turbulent flow. For instance, in the case of Kolmogorov turbulence $\lambda = \epsilon$ (ϵ is the kinetic energy flux); but for surface layer turbulence, the friction velocity v_* (and not the dissipation rate ϵ) becomes the only similarity parameter [13], $\lambda = {v_*}^2$ (therefore the expression $\lambda t^2 = (v_* t)^2$ provides the dimension of R^2).

The same dimensional analysis also leads to the important conclusion that the ballistic regime (and not the shear effect) is the universal long-time asymptote of the dispersion process of the tracer particle in the turbulent surface layer (see [14] and refs therein). This can be easily seen based on the following arguments. Let us assume that in addition to v_*, the problem is characterized by a length scale l (i.e. initial separation of the particles or the initial distance to the ground). Then the dimensional arguments translate (1) into

$$\langle R^2(t) \rangle \sim \lambda t^n, \quad \lambda = v_*^n l^{2-n}. \tag{4}$$

A naïve conjecture at this point would be that a dispersion mechanism with the highest value of n (e.g. shear) will dominate over large time periods (i.e. at $t \geq l/v_*$). However, more careful analysis casts doubt on this conclusion. Indeed, for $t \gg l/v_*$ particles should "forget" about their initial positions and the parameter l should be dropped from the expression for the particle separation (4) all together. We can see that the only possibility for this is the case when $n = 2$: conversion to the ballistic regime.

This variety of possible scenarios of tracer dispersion in the surface layer turbulence and some ambiguity of available analytical predictions (at least when being straightforwardly applied) motivated our experimental study of this phenomenon.

II. EXPERIMENTAL PROCEDURE

Scrutinizing measurements at a given location within the Taylor hypothesis of frozen turbulence $R = Ut$, where $U = const$; it follows from (1) that:

$$S_2(R) = 2[F_2(0) - F_2(R)] \propto R^{2/n} \propto (Ut)^{2/n}, \tag{5}$$

so single point time-measurements of concentration also show power-law behavior with the same characteristic exponents as the spatial measurements.

We estimated the value of parameter n in (5) based on extended atmospheric observations of the tracer concentrations. A continuous (and relatively stable) influx of particles into the turbulent flow was supplied by the anthropogenic activity in the surrounding urban areas (about 20 km in size). This "highly distributed" source of particles maintained the quasi-equilibrium (and on average, well mixed) tracer distribution which was validated by our long-term observations. The observation tower was at a height of $H = 12$m and the tracer concentration was measured by means of scattered light intensity off incoming particles. Continuous observation was undertaken over a period of 21 days with an air sample taken every 5 seconds (30 liters per sample). The instrumentation provided total particle count as well as their size distribution in the range of 1 - 10 μm. Local meteorological observations (three conventional meteorological stations in the vicinity) and global observations (with resolution about 1 km) were available to draw the conclusions about local meteorological conditions of the surface layer (stability, profiles of wind speed and temperature). Wind speed and temperature were also measured directly at the sampling point ($H = 12$m).

As usual in meteorological studies, we anticipated that the night time observations would correspond to the case of the boundary layer under stable or neutral conditions. For convective turbulence to be generated, an intensive heat flux from the underlying surface has to occur and this, of course, should include the significant effect of solar radiation. Indeed, in our experimental results the latter condition is bound to the daytime observations.

III. DATA ANALYSIS

Undertaking correlation analysis of the time series of the concentration $C(t)$, of single point measurements, we found that the minimum time span that provides reliable statistics of the process should be more than three hours. As the first step, we plotted $S_2(R)$ as a function of $R = Ut$ on a log-log scale and evaluated the scaling exponent n from the expression $S_2(R) \propto (Ut)^{2/n}$ predicted by (3) and (5). Some examples of these plots are depicted in Fig 1.

In this paper we report on the analysis of the data that corresponds to the stable conditions of the turbulent surface layer (results on convective tracer dispersion will be published elsewhere). As was mentioned above, the turbulent motion in this case is determined only by a one dimensional parameter - the friction velocity v_*, which provides the scale for velocity fluctuations. This

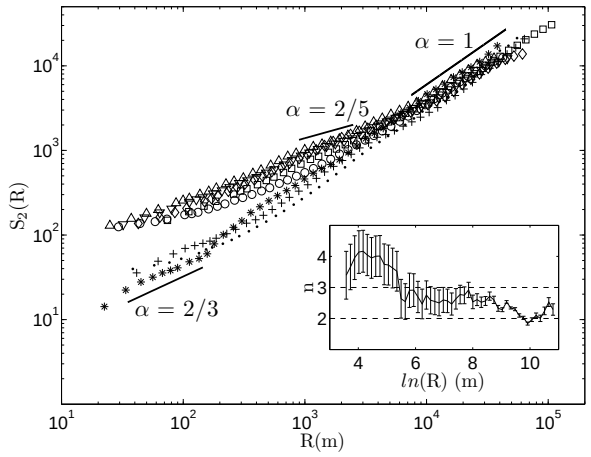

FIG. 1. Structure function of the tracer concentration $S_2(R) \propto R^\alpha \propto U_H t^\alpha$ on a log-log scale. Inset shows the estimation of how the scaling exponent of the mean inter particle displacement $\langle R^2(t)\rangle \propto t^n$ converges over time. Each data set corresponds to a maximum of 4 hours of observations and wind velocities outlined in Table I: +, Sample 1; ∘, Sample 2; ∗, Sample 3; ·, Sample 4; ⋄, Sample 5; □, Sample 6; ◊, Sample 7; △, Sample 8 and ▽, Sample 9. $\alpha = 2/3$ is the Richardson regime, $\alpha \approx 2/5$ is the velocity shear mechanism and $\alpha = 1$ is the ballistic regime. Global convergence to the ballistic regime ($\alpha = 1$) is clearly visible.

self-similarity property of the surface layer turbulence is expressed by the well-known relations [13]

$$\frac{\mathrm{d}U(z)}{\mathrm{d}z} = \frac{v_*}{\kappa z}, \quad \epsilon = \frac{v_*^3}{\kappa z}, \tag{6}$$

where z is the vertical distance from the underlying surface and ϵ is the dissipation rate, $\kappa = 0.4$.

The values of wind speed relevant to the data series depicted in Fig. 1 are listed in Table I. By using the logarithmic profile $U(z) = (v_*/\kappa) ln(z/z_0)$ followed from (6) we can estimate $v_* = cU_H$ ($c = \kappa/\ln(H/z_0)$) and then $\epsilon = v_*^3/\kappa z_0$. Assuming a typical value of roughness height $z_0 \approx 0.1$ m leads to to the estimates $c \approx 0.01$ and $\epsilon \approx 0.004$ kg m^2/s^3 for $U_H = 5.52$ m/s. The parameter $T_H \sim H/U(H) \sim H/cv_*$ corresponds to the time scale for a particle to reach the underlying surface and was of order 10^2 seconds.

The low relative fluctuations of the wind speed was one of the reasons that these data series were selected for analysis. It was also a justification for the application of the Taylor hypothesis to these datasets. It is worth noting that a particular value of the mean wind velocity has no relevance to the main reported result of our paper; it will only change the point at which a data series will approach the global asymptote in Fig. 1. It will not change either the existence of, nor the slope of this asymptote.

The dynamics of particle separation in the turbulence surface layer can be described by modifying the Langevin equation for particle separation [15]. By including the shear term proposed in [6] we can arrive at the following system:

TABLE I. Apropos mean wind speeds U_H for Fig. 1

Sample	U_H (m/s)
1.	4.15 ± 0.12
2.	2.94 ± 0.11
3.	2.25 ± 0.30
4.	3.85 ± 0.12
5.	5.52 ± 0.16
6.	7.42 ± 0.05
7.	4.27 ± 0.21
8.	2.49 ± 0.06
9.	3.20 ± 0.12

$$dR_x = G(R_z)dt + D(R)dt + \sqrt{2K}\ dW, \tag{7}$$

$$dR_\perp = D(R)dt + \sqrt{2K}\ dW, \tag{8}$$

where $G(R_z) = (dU/dz)R_z$ is the velocity shear term, $D(R) = (dK/dR + 2K/R)$ is the drift term, $K(R) = \beta\epsilon^{1/3}R^{4/3}$ is the diffusivity, $\beta = const$, $\epsilon(\mathbf{R})$ is the local dissipation flux (which describes the local activity of the turbulent flow) (6), dW is an isotropic Brownian motion, R_z is the vertical component of separation, R_x is its horizontal component and $\mathbf{R}_\perp = [R_z, R_y]$ are the components perpendicular to the mean shear; so $R^2 = R_x^2 + \mathbf{R}_\perp^2$.

For $t \ll T_H$, $U'(z) \sim v_*/\kappa H$, $\epsilon(\mathbf{R}) \approx \epsilon(H) = const$, so $G \ll D$. By placing $R_z \sim R_x \sim R_\perp \sim R$, we recover the standard Richardson regime $R^2 \propto t^3$ [6]. For the intermediate times ($t \approx T_H$) the velocity shear mechanism dominates ($G \gg D$) and following arguments of [6] we arrive at faster separation of particles ($R^2 \propto t^n$ with $4 \le n \le 6$). Finally, at the limiting case $t \ge T_H$ the separation becomes slower (ballistic with $R^2 \propto t^2$). The latter can be deduced from the system (7). At $t \gg T_H$ we can use estimates: $U'(z) \sim v_*/\kappa R_z$, $\epsilon(\mathbf{R}) = v_*^3/\kappa R_z$, which leads to a simplified system for the long-time asymptotes

$$dR_x \propto \sqrt{v_* R}\ dW, \quad dR_\perp \propto \sqrt{v_* R}\ dW, \tag{9}$$

since $R_z \sim R_\perp \sim R$.

We can see from the diffusive equation that the associated pdf $p(R,t)$ can be derived

$$\frac{\partial p}{\partial t} = \gamma v_* \frac{\partial}{\partial R}\left(R\frac{\partial p}{\partial R}\right), \tag{10}$$

where γ is the constant of order of unity. This equation has a straightforward solution:

$$p(R,t) = \frac{1}{2\gamma v_* t}\exp\left(-\frac{R}{\gamma v_* t}\right). \tag{11}$$

It is evident from here that the main asymptote of the model as $t \to \infty$ is the ballistic regime $\langle R(t)\rangle = \int_0^\infty Rp(R,t)\mathrm{d}R \sim v_* t$.

The existence of this global ballistic asymptote often suppresses the effect of the shear dispersion and clearly emerges from our experimental data (see Fig 1). We observe that at the short-time intervals, close to $t = 0$, the parameter $n \approx 3$ (Richardson regime), then it reaches maximum: $n \approx 5$ (shear dispersion) and finally n gradually decays to the the ballistic value: $n \approx 2$. It is worth noting that the long-time ballistic limit $n \approx 2$ is in agreement with recent experimental data on atmospheric dispersion $2 \leq n < 3$, see [14], [12] and references therein.

The non-trivial scaling properties of tracer dispersion in the turbulent surface layer can be also demonstrated by means of exit-time statistics for the concentration time series [8]; which are statistics of time intervals in which a measured value of concentration exits through a set of thresholds. By scanning the time series for a given threshold δC, one can recover a set of times $\tau_i(\delta C)$, where the measured concentration reaches this threshold. This set can then be used to calculate the Inverse Structure Function (for details see [8], [10]):

$$\Sigma_q(\delta C) \equiv \langle \tau^q(\delta C) \rangle. \tag{12}$$

A comprehensive analysis of the properties of the Inverse Structure Function can be fulfilled by applying the well-known mutifractal approach [8], [16]. This results in the following scaling [8], [16]:

$$\Sigma_q(\delta C) \propto (\delta C)^{\chi(q)}, \quad \chi(q) = \min_h [(q + 3 - D(h))/h] \tag{13}$$

where h is the index of singularity from the range $[h_{min}, h_{max}]$ such that $t \sim (\delta C)^h$ and $D(h)$ is the fractal dimension of the set with a singularity h. It is worth noting that particular values $h = 1/3$, $h = 1/5$ and $h = 1/2$ correspond to the Richardson law, the shear dispersion and the ballistic scaling discussed above.

According to [16], the function $(q+3-D(h))/h$ reaches its minimum at the upper boundary of the singularities' range, so we can set $h = h_{max}$ and write

$$\chi(q) = (q + 3 - D(h_{max}))/h_{max}. \tag{14}$$

This leads to the important conclusion that $\chi(q)$ is a linear function of q (i.e. no intermittency correction), which has been verified by numerical simulations and by some limited experimental data [16]. This conclusion was also validated against our experimental dataset and the results are shown in Fig 2. We observe that indeed $\chi(q)$ closely follows the predicted linear trend for $q \geq 1$ and provides a reasonable match with the experimental data available in the literature [17]. A change in slope near the value $q = 1$ can be attributed to a contribution of the slow (differentiable) components of turbulent motion [10]. A model for this effect will be discussed elsewhere.

We also present a plot of the mean exit-time $\Sigma_1(\delta C) = \langle t(\delta C) \rangle$ as a function of the concentration threshold δC in Fig 3. C_0 and its associated t_0 are located at the concentration minima for each sample, and are used to collapse data only. Three asymptotes corresponding to the regimes discussed above are also depicted for comparison. These asymptotes can be easily established from (5) based on simple dimensional arguments. Indeed, for the short times $t \ll T_H$ we can assume Richardson (or Corsin-Obukhov) scaling $\delta C \propto t^{1/3}$ and derive $\langle t(\delta C) \rangle \propto (\delta C)^3$. Similarly, for the shear dispersion we can write $\langle t(\delta C) \rangle \propto (\delta C)^n, n \approx 5$ [6]; while for the ballistic regime at the longer times ($t \gg T_H$) we arrive at the scaling $\langle t(\delta C) \rangle \propto (\delta C)^2$. A subsequent change of regime as discussed above, corresponding to the curve $\langle t(\delta C) \rangle$ deviating from one asymptote to another, is clearly visible. From this plot it is also evident why in the case of wall-bounded turbulent dispersion it is not possible to assign any universal value for parameter n in the scaling law $\langle t(\delta C) \rangle \propto (\delta C)^n$ (similarly in (2)), which is in agreement with the conclusions of [9].

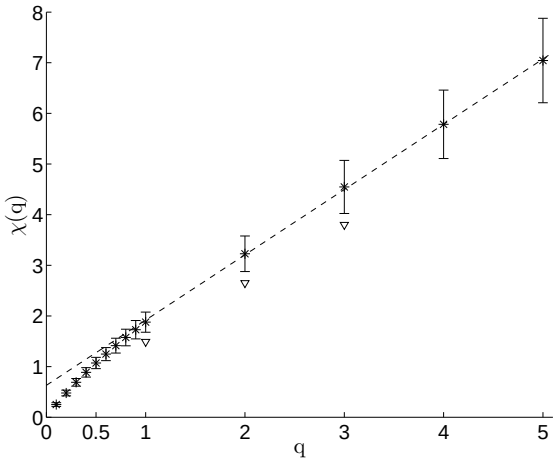

FIG. 2. Mean Inverse Structure Function for 12 experimental data sets (∗). Error bars correspond to ± mean standard deviation. The dashed line represents a linear best fit over $1 \leq q \leq 5$ predicted by (14) [16]. Experimental values for temperature fluctuations (▽) of [17] are presented for reference.

IV. CONCLUSIONS

We presented experimental results for passive tracer dispersion in the turbulent surface layer under stable conditions. In this case the dispersion of tracer particles was affected by the mean velocity gradient and flow boundaries. We found that our observations can be intrinsically explained with the three-stage model of tracer dispersion. During the first stage of separation ($T \ll H/v_*$, where H is the observation height and v_* is the friction velocity) tracer particles obey the standard Richardson model. During the second stage ($T \approx H/v_*$) the shear mechanism of dispersion dominates [6]. Finally, when ($T \gg H/v_*$) the shear mechanism is followed by a transition to the ballistic regime of dispersion induced by the

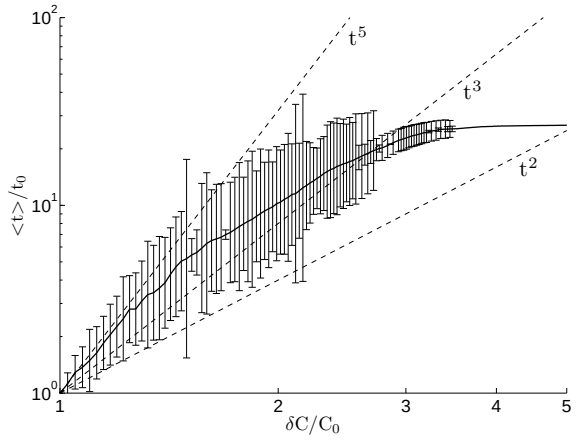

FIG. 3. Exit-time for the first moment of the concentration time series. Different regimes of dispersion correspond to the different power-law asymptotes (see text). Scaling factors C_0, t_0 were used for collapsing data thus a better visual appearance (see text).

specific scaling properties of the turbulence in the surface layer. This scenario of inter-particle distance seems to be in agreement with atmospheric observations [14], [12] as well as experimental results on tracer dispersion by turbulent surface flow in water channels [18]. We found that the ballistic regime always suppressed the velocity-shear effect predicted in [6] at the later stage of dispersion, resulting in much slower rate of particle separation (i.e. lower value of parameter n in (1)). Exit-time statistics were derived from the experimental dataset and showed a reasonable match with the simple dimensional asymptotes, as well as predictions of the multifractal model and experimental data from other sources.

[1] U. Frisch, *Turbulence. The legacy of A. N. Kolmogorov* (Cambridge Univ. Press, 1995).
[2] B. Shraiman and E. Siggia, Nature **405**, 639 (2000).
[3] G. Falkovich, K. Gawedzki, and M. Vergassola, Rev. Mod. Phys. **73**, 913 (2001).
[4] J. Duplat and E. Villermaux, J. Fluid Mech. **617**, 51 (2008).
[5] A. Celani, M.Cencini, A. Mazzino, and M. Vergassola, New J. Phys. **6**, 72 (2004).
[6] A. Celani, M. Cencini, M. Vergassola, E. Villermaux, and D. Vincenzi, J. Fluid Mech. **523**, 99 (2005).
[7] G. Gioia, G. Lacorata, E. P. M. Filho, A. Mazzino, and U. Rizza, Boundary-Layer Meteorology **113**, 187 (2004).
[8] G. Boffetta, A. Mazzino, and A. Vulpiani, J. Phys. A **41**, 363001:25 (2008).
[9] V. Lebedev and K. Turitsyn, Phys. Rev. E **69**, 036301:11 (2004).
[10] A. Bistagnino and G. Boffetta, New J. Phys. **10**, 075018 (2008).
[11] L. Richardson, Proc. R. Soc. Lond. A **110**, 709 (1926).
[12] J. Salazar and L. Collins, Annu. Rev. Fluid Mech. **41**, 405 (2009).
[13] A. Monin and A. Yaglom, *Statistical Fluid Mechanics, Vol. 1&2* (Cambridge: MIT Press, 1975).
[14] T. Mikkelsen, H. Jørgensen, M. Nielsen, and S. Ott, Boundary-Layer Meteorology **105**, 483 (2002).
[15] B. Sawford, J. Turbulence **7**, 13 (2006).
[16] F. Schmitt, Phys. Lett. A **342**, 448 (2005).
[17] S. Beaulac and L. Mydlarski, Phys. Fluids **16**, 2126 (2004).
[18] M. Borgas, R. Gailis, A. Skvortsov, and V. Bisignanesi, (to be published).